Electronic Supplementary Material (ESI) for Dalton Transactions.

Supporting Information

Synthesis of Atomically Precise Single-Crystalline Ru_2-Based Coordination Polymers

Wen-Yang Gao,[†] Gerard Pierre Van Trieste III,[†] and David C. Powers*[†]

[†]*Department of Chemistry, Texas A&M University, College Station, Texas 77843, United States*

Email: powers@chem.tamu.edu

Table of Contents

A. General Considerations

Materials Unless otherwise noted, all chemicals and solvents (ACS reagent grade) were used as received. 4-Cyanobenzoic acid was obtained from TCI. Methanol (MeOH), diethyl ether (Et_2O), tetrahydrofuran (THF), acetone, hexanes, acetonitrile (MeCN), 3-cyanobenzoic acid, 2-aminopyridine-4-carbonitrile, and silver trifluoromethanesulfonate (AgOTf) were obtained from Sigma Aldrich. Chlorobenzene was obtained from Bean Town Chemical. Silver tetrafluoroborate ($AgBF_4$) was purchased from Strem Chemicals, Inc. 2-Hydroxyisonicotinonitrile was purchased from Matrix Scientific. $Ru_2(OAc)_4Cl$[1] and 3,5-dicyanobenzoic acid[2] were prepared according to literature methods. NMR solvents were purchased from Cambridge Isotope Laboratories and were used as received. All reactions were carried out under ambient atmosphere unless otherwise noted.

Characterization Details NMR spectra were recorded on a Bruker Ascend 400 operating at 400.13 MHz for ^1H acquisition or a Varian NMRS 500RM operating at 500.13 MHz for ^1H acquisition. Spectra were referenced against residual proton solvent resonances: *d*$_6$-acetone (2.05 ppm, ^1H) and *d*$_6$-DMSO (2.50 ppm, ^1H).[3] ^1H NMR data are reported as follows: chemical shift (δ, ppm), (multiplicity: s (singlet), d (doublet), t (triplet), m (multiplet), br (broad); integration). IR spectra were recorded on ATI Mattson Genesis Series FTIR with ATR spectrometer. Spectra were blanked against air and were determined as the average of 32 scans. IR data are reported as follows: wavenumber (cm^{-1}), (peak intensity: s, strong; m, medium; w, weak). Matrix-assisted laser desorption ionization (MALDI) data were obtained using a Bruker Microflex LRF MALDI-TOF using reflectron-TOF modes.

X-ray Diffraction Details Single-crystal X-ray diffraction (SCXRD) data of Ru_2(4-CN-OBz)$_4BF_4$ (**2a**), [Ag(**2a**)OTf], [Ag_2(**2b**)$(OTf)_2$], and [Ag_2(**2d**)$(OTf)_2$] were collected using a Bruker ApexII CCD area detector diffractometer equipped with sealed tube Mo (Mo K_α = 0.71073 Å) operating at 110 K. SCXRD data of [Ag_2(**2c**)$(OTf)_2$] were collected using synchrotron radiation (λ = 0.41328 Å) equipped with a Pilatus3 X CdTe 1M detector and an Oxford cryostream cooling device operating at 110 K at NSF's ChemMatCARS Sector 15 of Advanced Photon Source (APS) housed at Argonne National Laboratory (ANL). SCXRD data of [Ag_2(**2e**)$(OTf)_2$] were collected using a Bruker Quest CPAD area detector diffractometer equipped with microfocus molybdenum source lμS (Mo K_α = 0.71073 Å) operating at 110 K. Indexing was performed using Bruker APEX2. Data integration and reduction were performed using SaintPlus. Absorption corrections were performed by the multi-scan method implemented in SADABS.[4] Space group determinations were carried out using XPREP implemented in APEX2. Structures were solved using SHELXT and refined using SHELXL-2017 (full-matrix least-squares on F^2)[5-6] using the OLEX2 interface.[7] All non-hydrogen atoms were refined anisotropically. Hydrogen atoms were placed at idealized positions and refined using a riding model. Solvent masks were employed in OLEX2 to treat the disorder solvents (e.g. acetone and hexane) in the cavities.

Powder X-ray diffraction (PXRD) measurements were carried out on a Bruker D8 Advance Eco X-ray diffractometer (Cu Kα, 1.5418 Å; 40 kV, 25 mA) fitted with a LynxEye detector. The angular range was measured from 5.00 to 30.00° (2θ) with steps of 0.020° and a measurement time of 0.3 second per step. Simulated PXRD patterns were calculated using Mercury 3.9.[8]

B. Synthesis and Characterization

Synthesis of Ru_2(4-CN-OBz)$_4BF_4$ (2a)

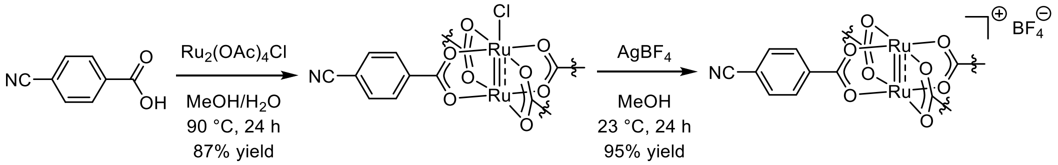

A 50-mL round bottom flask was charged with $Ru_2(OAc)_4Cl$ (0.150 g, 0.317 mmol, 1.00 equiv), 4-cyanobenzoic acid (0.280 g, 1.90 mmol, 6.00 equiv), MeOH (5.0 mL), and H_2O (5.0 mL). With stirring, the reaction mixture was heated to reflux for 24 h. The reaction mixture was cooled to 23 °C and the obtained precipitate was collected by vacuum filtration. The solids were extensively washed with a mixture of MeOH and Et_2O (v/v=1:2, 9 mL × 3) to remove unreacted 4-cyanobenzoic acid and the solids were dried under reduced pressure to afford Ru_2(4-CN-OBz)$_4$Cl (**1a**, 0.226 g, 87% yield) as a light orange solid. IR (cm^{-1}, Figure S1): 2228 (w), 1617 (w), 1506 (w), 1458 (w), 1407 (s), 1294 (w), 1179 (w), 1140 (w), 1017 (w), 861 (w), 763 (m), 692 (m), 607 (m). ^{1}H NMR (δ, 23 °C, *d*$_6$-DMSO, Figure S13): 30.9 (br, 2H), 7.9 (br, 2H). Mass spectrometry (MALDI, positive): calc ($[Ru_2(C_8H_4NO_2)_4]^+$): 787.91; expt: m/z = 787.95.

A 50-ml round bottom flask was charged with **1a** (0.200 g, 0.243 mmol, 1.00 equiv), $AgBF_4$ (0.047 g, 0.243 mmol, 1.00 equiv), and MeOH (20.0 mL). The reaction mixture was stirred at 23 °C for 24 h in the dark. The reaction mixture was filtered through a Celite plug and the filtrate was concentrated under reduced pressure to afford the title compound (Ru_2(4-CN-OBz)$_4BF_4$, **2a**) as an orange solid (0.202 g, 95% yield). Crystals of Ru_2(4-CN-OBz)4BF4 suitable for SCXRD analysis were obtained by slow evaporation of a saturated acetone solution at 23 °C. IR (cm^{-1}, Figure S1): 2258 (w), 2228 (w), 1630 (w), 1504 (w), 1457 (w), 1406 (s), 1296 (w), 1199 (w), 1182 (w), 1141 (w), 1035 (m), 1016 (m), 859 (m), 763 (m), 691 (m), 614 (m). ^{1}H NMR (δ, 23 °C, *d*$_6$-acetone, Figure S14): 31.5 (br, 2H), 7.7 (br, 2H).

Synthesis of Ru_2(3-CN-OBz)$_4BF_4$ (2b)

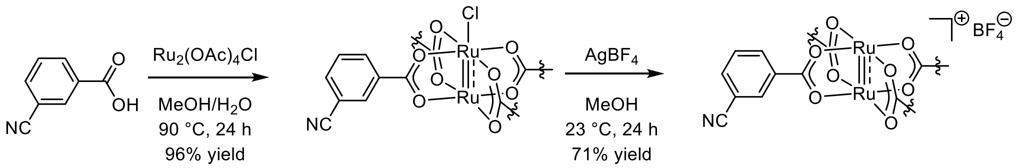

A 50-mL round bottom flask was charged with $Ru_2(OAc)_4Cl$ (0.150 g, 0.317 mmol, 1.00 equiv), 3-cyanobenzoic acid (0.280 g, 1.90 mmol, 6.00 equiv), MeOH (5.0 mL), and H_2O (5.0 mL). With stirring, the reaction mixture was heated to reflux for 24 h. The reaction mixture was cooled to 23 °C and the obtained precipitate was collected by vacuum filtration. The solids were extensively washed with a mixture of MeOH and Et_2O (v/v=1:2, 9 mL × 3) to remove unreacted 3-cyanobenzoic acid and the solids were dried under reduced pressure to afford Ru_2(3-CN-OBz)$_4$Cl (**1b**, 0.250 g, 96% yield) as a light orange solid. IR (cm^{-1}, Figure S2): 2231 (w), 1603 (w), 1462 (m), 1426 (m), 1396 (s), 1210 (w), 1091 (w), 999 (w), 912 (w), 822 (w), 782 (m), 755 (m), 676 (s), 566 (w). ^{1}H NMR (δ, 23 °C, *d$_6$*-DMSO, Figure S15): 30.7 (br, 2H), 19.2 (br, 1H), 7.4 (br, 1H). Mass spectrometry (MALDI, positive): calc ([$Ru_2(C_8H_4NO_2)_4$]$^+$): 787.91; expt: m/z = 787.88.

A 50-ml round bottom flask was charged with **1b** (0.200 g, 0.243 mmol, 1.00 equiv), $AgBF_4$ (0.047 g, 0.243 mmol, 1.00 equiv), and MeOH (20.0 mL). The reaction mixture was stirred at 23 °C for 24 h in the dark. The reaction mixture was filtered through a Celite plug and the filtrate was concentrated under reduced pressure to afford the title compound (Ru_2(3-CN-OBz)$_4BF_4$, **2b**) as an orange solid (0.150 g, 71% yield). IR (cm^{-1}, Figure S2): 2265 (w), 1641 (w), 1606 (w), 1532 (w), 1465 (w), 1424 (m), 1395 (s), 1287 (w), 1214 (w), 1176 (w), 1023 (s), 823 (w), 787 (m), 756 (m), 676 (m), 599 (w), 564 (w).^{1}H NMR (δ, 23 °C, *d$_6$*-acetone, Figure S16): 31.4 (br, 2H), 19.6 (br, 1H), 7.8 (br, 1H). Mass spectrometry (MALDI, positive): calc ([$Ru_2(C_8H_4NO_2)_4$]$^+$): 787.76; expt: m/z = 787.88.

Synthesis of Ru$_2$(3,5-diCN-OBz)$_4$BF$_4$ (2c)

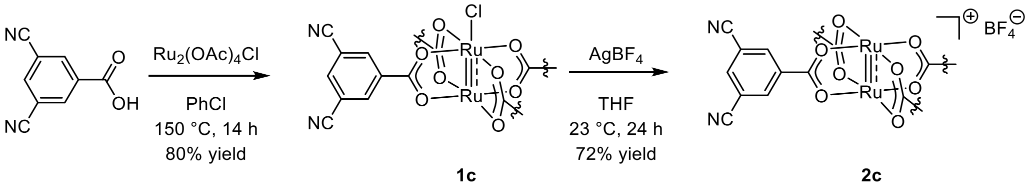

A 50-mL round bottom flask was charged with $Ru_2(OAc)_4Cl$ (0.144 g, 0.304 mmol, 1.00 equiv), 3,5-dicyanobenzoic acid (0.235 g, 1.37 mmol, 4.50 equiv), and chlorobenzene (30.0 mL). With stirring, the reaction mixture was heated to reflux for 24 h. The reaction mixture was cooled to 23 °C and the solvent was removed under reduced pressure. The solids were extensively washed with Et_2O (10.0 mL × 3) to remove unreacted 3,5-dicyanobenzoic acid and the solids were dried under reduced pressure to afford Ru_2(3,5-diCN-OBz)$_4$Cl (**1c**, 0.224 g, 80% yield) as a light orange solid. IR (cm^{-1}, Figure S3): 2241 (w), 1719 (w), 1670 (w), 1612 (w), 1562 (w), 1501 (w), 1440 (m), 1393 (s), 1292 (w), 1259 (w), 1211 (w), 1115 (w), 914 (w), 763 (s), 730 (s), 696 (m), 671 (m). The obtained solid was used for the following step without further purification.

A 50-ml round bottom flask was charged with **1c** (0.200 g, 0.217 mmol, 1.00 equiv), $AgBF_4$ (0.042 g, 0.217 mmol, 1.00 equiv), and THF (30.0 mL). The reaction mixture was stirred at 23 °C for 24 h in the dark. The reaction mixture was filtered through a Celite plug and the filtrate was concentrated under reduced pressure to afford the title compound (Ru_2(3,5-diCN-OBz)$_4BF_4$, **2c**) as an orange solid (0.152 g, 72% yield). IR (cm^{-1}, Figure S3): 2260 (w), 2245 (w), 1723 (w), 1627 (w), 1482 (w), 1446 (m), 1398 (s), 1311 (w), 1260 (m), 1232 (w), 1215 (w), 1156 (w), 1022 (s), 912 (w), 860 (w), 796 (m), 760 (s), 726 (s), 702 (m), 667 (m). ^{1}H NMR (δ, 23 °C, *d$_6$*-acetone, Figure S17): 31.2 (br, 2H), 20.1 (br, 1H).

Synthesis of Ru_2(4-CN-ap)$_4BF_4$ (2d)

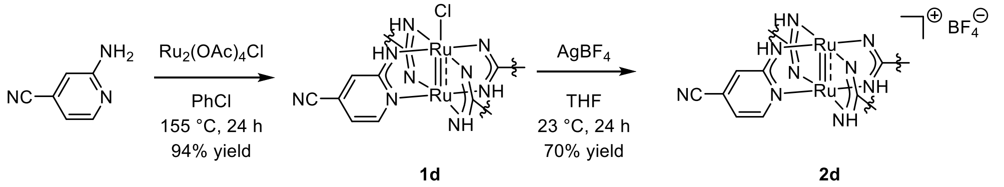

A 50-mL round bottom flask was charged with $Ru_2(OAc)_4Cl$ (0.131 g, 0.277 mmol, 1.00 equiv), 2-aminopyridine-4-carbonitrile (0.166 g, 1.39 mmol, 5.02 equiv), and chlorobenzene (20.0 mL). With stirring, the reaction mixture was heated to reflux for 24 h. The reaction mixture was cooled to 23 °C and the obtained precipitate was collected by vacuum filtration. The solids were extensively washed with MeOH (9.0 mL × 3) to remove unreacted 2-aminopyridine-4-carbonitrile and the solids were dried under reduced pressure to afford Ru_2(4-CN-ap)$_4$Cl (**1d**, 0.185 g, 94% yield) as a dark green solid. IR (cm^{-1}, Figure S4): 2235 (w), 1605 (m), 1522 (w), 1441 (s), 1389 (s), 1354 (m), 1318 (m), 1271 (m), 1214 (w), 1155 (w), 1011 (m), 948 (m), 848 (m), 785 (m), 755 (m), 688 (s), 641 (s).

A 50-ml round bottom flask was charged with **1d** (0.160 g, 0.225 mmol, 1.00 equiv), $AgBF_4$ (0.044 g, 0.225 mmol, 1.00 equiv), and THF (20.0 mL). The reaction mixture was stirred at 23 °C for 24 h in the dark. The reaction mixture was filtered through a Celite plug and the filtrate was concentrated under reduced pressure to afford the title compound (Ru_2(4-CN-ap)$_4BF_4$, **2d**) as a dark green solid (0.120 g, 70% yield). IR (cm^{-1}, Figure S4): 2235 (w), 1771 (m), 1719 (m), 1607 (w), 1545 (w), 1464 (w), 1418 (w), 1372 (w), 1323 (w), 1277 (w), 1169 (m), 1032 (s), 989 (s), 921 (m), 865 (w), 793 (w), 692 (w), 640 (w).

Synthesis of Ru_2(4-CN-hp)$_4BF_4$ (2e)

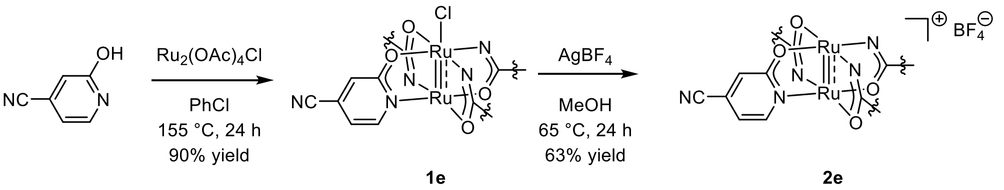

A 50-mL round bottom flask was charged with $Ru_2(OAc)_4Cl$ (0.200 g, 0.422 mmol, 1.00 equiv), 2-hydroxyisonicotinonitrile (0.223 g, 1.86 mmol, 4.40 equiv), and chlorobenzene (30.0 mL). With stirring, the reaction mixture was heated to reflux for 24 h. The reaction mixture was cooled to 23 °C and the obtained precipitate was collected by vacuum filtration. The solids were extensively washed with MeOH (9.0 mL × 3) to remove unreacted 2-hydroxyisonicotinonitrile and the solids were dried under reduced pressure to afford Ru_2(4-CN-hp)$_4$Cl (**1e**, 0.271 g, 90% yield) as a dark brown solid. IR (cm^{-1}, Figure S5): 2235 (w), 1649 (w), 1606 (m), 1519 (w), 1466 (m), 1430 (s), 1323 (w), 1276 (w), 1228 (w), 1149 (w), 1016 (w), 1001 (w), 959 (m), 857 (m), 803 (m), 790 (w), 753 (w), 739 (w), 699 (w), 649 (m), 636 (m), 621 (m). Mass spectrometry (MALDI, positive): calc ($[Ru_2(C_6H_3N_2O)_4]^+$): 679.91; expt: m/z = 679.95.

A 50-ml round bottom flask was charged with **1e** (0.200 g, 0.300 mmol, 1.00 equiv), $AgBF_4$ (0.058 g, 0.30 mmol, 1.0 equiv), and MeOH (20.0 mL). With stirring, the reaction mixture was heated to reflux for 24 h in the dark. The reaction mixture was cooled to 23 °C and the reaction mixture was filtered through a Celite plug. The filtrate was concentrated under reduced pressure to afford the title compound (Ru_2(4-CN-hp)$_4$$BF_4$, **2e**) as a dark brown solid (0.14 g, 63% yield). IR (cm^{-1}, Figure S5): 2266 (w), 1617 (m), 1523 (w), 1468 (w), 1428 (m), 1327 (w), 1288 (w), 980 (s), 764 (m), 671 (m), 644 (m).

Synthesis of Heterobimetallic Coordination Polymers

Synthesis of [Ag(2a)OTf][a]

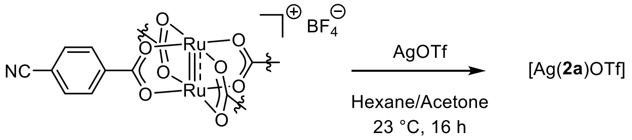

2a

A 1.0-dram borosilicate vial was charged with **2a** (13 mg, 0.015 mmol, 1.0 equiv), AgOTf (15 mg, 0.060 mmol, 4.0 equiv), and acetone (1.2 mL). The resulting mixture was sonicated for 3 min, which resulted in a clear solution. Hexanes (2.5 mL) was carefully layered on the top. The vial was sealed with a screw cap and left undisturbed at 23 °C in the dark. Dark orange single crystals of [Ag(**2a**)OTf] suitable for X-ray diffraction analysis were obtained after 16 h. IR (cm^{-1}, Figure S12a): 2254 (w), 1694 (w), 1635 (w), 1608 (w), 1577 (w), 1504 (w), 1455 (m), 1406 (s), 1279 (w), 1234 (m), 1178 (w), 1168 (w), 1141 (w), 1054 (m), 1022 (s), 860 (w), 765 (s), 693 (m), 636 (m), 611 (m), 547 (m).

Synthesis of [Ag_2(2b)($OTf)_2$]

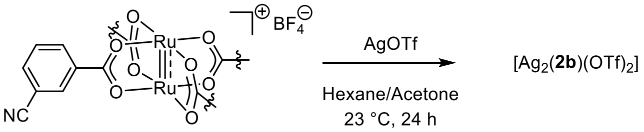

2b

A 1.0-dram borosilicate vial was charged with **2b** (13 mg, 0.015 mmol, 1.0 equiv), AgOTf (15 mg, 0.060 mmol, 4.0 equiv), and acetone (1.0 mL). The resulting mixture was sonicated for 3 min, which resulted in a clear solution. Hexanes (3.0 mL) was carefully layered on the top. The vial was sealed with a screw cap and left undisturbed at 23 °C in the dark. Dark orange single crystals of [Ag_2(**2b**)($OTf)_2$] suitable for X-ray diffraction analysis were obtained after 24 h. IR (cm^{-1}, Figure S12b): 2260 (w), 1629 (w), 1605 (w), 1482 (w), 1466 (w), 1427 (m),

---

[a] The following is representative of attempts to prepare [Ag(**2a**)OTf] via solvothermal methods. A 20 mL borosilicate vial was charged with $Ru_2(OAc)_4Cl$ (7.1 mg, 0.015 mmol, 1.0 equiv), 4-cyanobenzoic acid (9.5 mg, 0.065 mmol, 4.3 equiv), AgOTf (16 mg, 0.062 mmol, 4.1 equiv), and acetone (1.0 mL). The resulting mixture was sonicated for 3 min. The vial was sealed with a screw cap and left undisturbed at 80 °C in the oven. Silver mirror was observed after 36 h. Silver mirror was also observed, when the reaction was conducted with compound **2a**. A 20 mL borosilicate vial was charged with **2a** (13 mg, 0.015 mmol, 1.0 equiv), AgOTf (15 mg, 0.060 mmol, 4.0 equiv), and acetone (1.0 mL). The resulting mixture was sonicated for 3 min, which resulted in a clear solution. The vial was sealed with a screw cap and left undisturbed at 80 °C in the oven. Silver mirror was observed after 36 h. No other solids were observed.

1396 (s), 1270 (m), 1239 (m), 1226 (m), 1173 (w), 1057 (m), 1023 (s), 916 (w), 822 (w), 787 (m), 756 (m), 736 (w), 703 (w), 676 (m), 637 (m), 603 (w), 565 (w).

Synthesis of [Ag$_2$(2c)(OTf)$_2$][b]

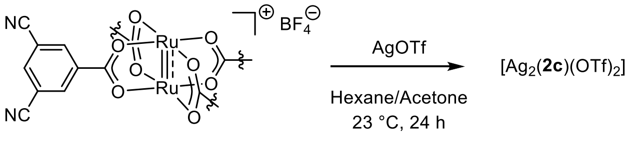

2c

A 1.0-dram borosilicate vial was charged with **2c** (10 mg, 0.010 mmol, 1.0 equiv), AgOTf (10 mg, 0.040 mmol, 4.0 equiv), and acetone (0.5 mL). The resulting mixture was sonicated for 3 min, which resulted in a clear solution. Hexanes (2.0 mL) was carefully layered on the top. The vial was sealed with a screw cap and left undisturbed at 23 °C in the dark. Dark orange single crystals of [Ag$_2$(**2c**)(OTf)$_2$] suitable for X-ray diffraction analysis were obtained after 24 h. See Figures S8b and 8c for topological analysis. IR (cm^{-1}, Figure S12c): 3083 (w), 2259 (w), 1687 (w), 1673 (w), 1625 (w), 1598 (w), 1483 (w), 1447 (m), 1399 (s), 1278 (m), 1256 (m), 1236 (m), 1223 (m), 1163 (m), 1059 (m), 1025 (s), 933 (w), 910 (w), 761 (s), 705 (w), 668 (m), 636 (m), 595 (w), 543 (w).

Synthesis of [Ag$_2$(2d)(OTf)$_2$]

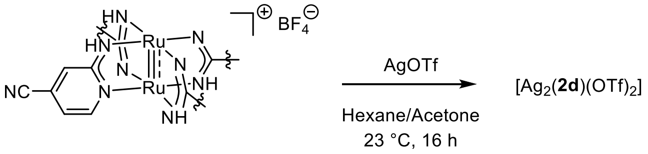

2d

A 1.0-dram borosilicate vial was charged with **2d** (12 mg, 0.015 mmol, 1.0 equiv), AgOTf (15 mg, 0.060 mmol, 4.0 equiv), and acetone (1.0 mL). The resulting mixture was sonicated for 3 min, which resulted in a clear solution. Hexanes (2.5 mL) was carefully layered on the top. The vial was sealed with a screw cap and left undisturbed at 23 °C in the dark. Dark green single crystals of [Ag$_2$(**2d**)(OTf)$_2$] suitable for X-ray diffraction analysis were obtained after 24 h. IR (cm^{-1}, Figure S12d): 2260 (w), 1690 (w), 1610 (m), 1522 (w), 1450 (s), 1372 (w), 1327 (w), 1263 (m), 1217 (s), 1164 (s), 1130 (m), 1090 (w), 1019 (s), 956 (m), 874 (w), 798 (w), 761 (w), 733 (w), 672 (w), 632 (m), 603 (w).

Synthesis of [Ag$_2$(2e)(OTf)$_2$]

---

[b] The following is representative of attempts to prepare [Ag$_2$(**2c**)(OTf)$_2$] via solvothermal methods. A 20 mL borosilicate vial was charged with **2c** (11 mg, 0.011 mmol, 1.0 equiv), AgOTf (13 mg, 0.051 mmol, 4.6 equiv), and acetone (1.0 mL). The resulting mixture was sonicated for 3 min, which resulted in a clear solution. The vial was sealed with a screw cap and left undisturbed at 80 °C in the oven. Silver mirror was observed after 36 h. No other solids were observed.

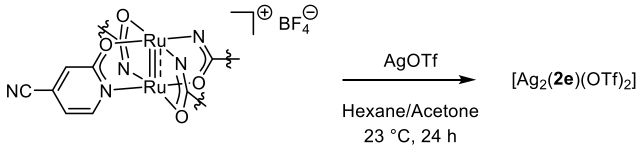

2e

A 2.0-dram borosilicate vial was charged with **2e** (10 mg, 0.015 mmol, 1.0 equiv), AgOTf (15 mg, 0.060 mmol, 4.0 equiv), and acetone (2.0 mL). The resulting mixture was sonicated for 3 min, which resulted in a clear solution. Hexanes (3.0 mL) was added to the mixture. The resulting solution was filtered through Celite. Hexane (2.0 mL) was carefully layered on the top. The vial was sealed with a screw cap and left undisturbed at 23 °C in the dark. Dark red single crystals of [Ag_2(**2e**)$(OTf)_2$] suitable for X-ray diffraction analysis were obtained after 24 h. IR (cm^{-1}, Figure S12e): 3114 (w), 2959 (w), 2265 (w), 1680 (w), 1639 (m), 1598 (m), 1509 (w), 1471 (w), 1415 (w), 1367 (w), 1275 (m), 1218 (s), 1167 (s), 1089 (w), 1022 (s), 882 (w), 795 (w), 763 (w), 713 (w), 633 (m), 604 (w).

MeCN Exposure Experiments

Single-crystalline samples of [Ag(**2a**)OTf], [Ag_2(**2b**)$(OTf)_2$], [Ag_2(**2c**)$(OTf)_2$], [Ag_2(**2d**)$(OTf)_2$], and [Ag_2(**2e**)$(OTf)_2$] were obtained by decanting the solvent from the reaction vials used to crystallize these materials (~5 mg for each). MeCN (1.0 mL) was added to each solid sample. The solid sample of coordination polymers dissolved in MeCN immediately, which indicates the coordination polymers are not stable toward MeCN.

C. Supporting Data

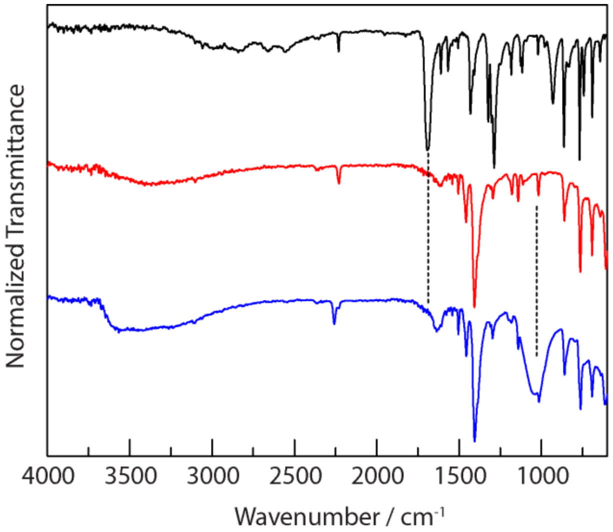

Figure S1. IR spectra of 4-cyanobenzoic acid (—), $Ru_2(4\text{-CN-OBz})_4Cl$ (**1a**, —), and $Ru_2(4\text{-CN-OBz})_4BF_4$ (**2a**, —). The carbonyl stretching frequency of 4-cyanobenzoic acid (~1690 cm^{-1}) disappears after thermally promoted ligand exchange with $Ru_2(OAc)_4Cl$. The characteristic B–F stretching frequency of tetrafluoroborate anion (broad ~1020 cm^{-1}) is observed after treatment of **1a** with $AgBF_4$.

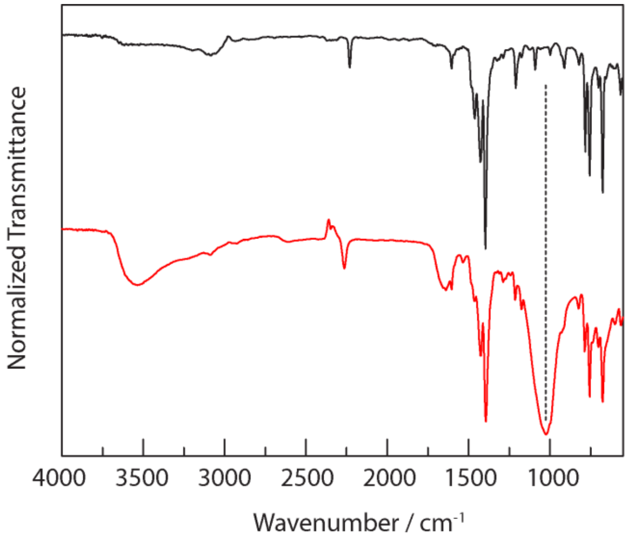

Figure S2. IR spectra of Ru$_2$(3-CN-OBz)$_4$Cl (**1b**, —) and Ru$_2$(3-CN-OBz)$_4$BF$_4$ (**2b**, —). The characteristic B–F stretching frequency of tetrafluoroborate anion (broad ~1020 cm^{-1}) is observed after treatment of **1b** with AgBF$_4$.

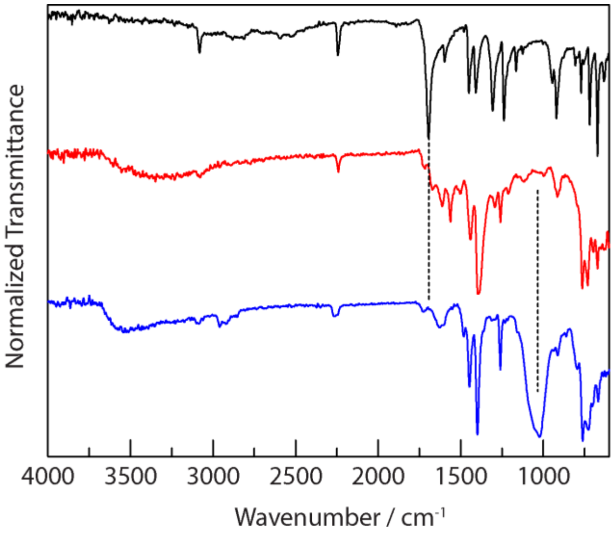

Figure S3. IR spectra of 3,5-dicyanobenzoic acid (—), Ru$_2$(3,5-diCN-OBz)$_4$Cl (**1c**, —), and Ru$_2$(3,5-diCN-OBz)$_4$BF$_4$ (**2c**, —). The carbonyl stretching frequency of 3,5-dicyanobenzoic acid (~1690 cm^{-1}) disappears after thermally promoted ligand exchange with Ru$_2$(OAc)$_4$Cl. The characteristic B–F stretching frequency of tetrafluoroborate anion (broad ~1020 cm^{-1}) is observed after treatment of **1c** with AgBF$_4$.

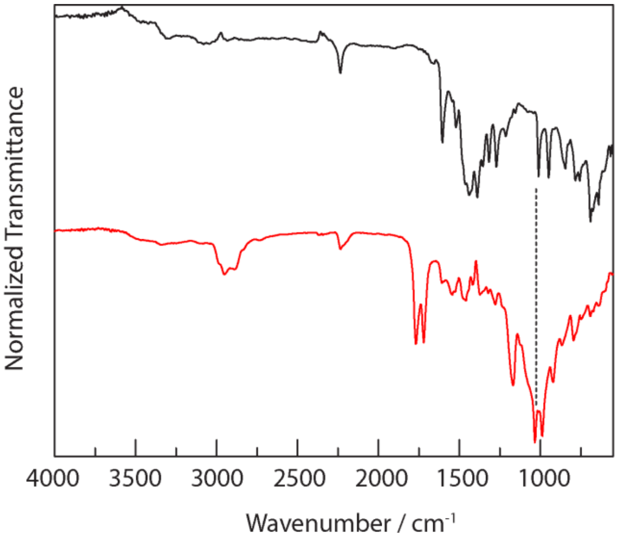

Figure S4. IR spectra of Ru$_2$(4-CN-ap)$_4$Cl (**1d**, —) and Ru$_2$(4-CN-ap)$_4$BF$_4$ (**2d**, —). The characteristic B–F stretching frequency of tetrafluoroborate anion (broad ~1020 cm^{-1}) is observed after treatment of **1d** with AgBF$_4$.

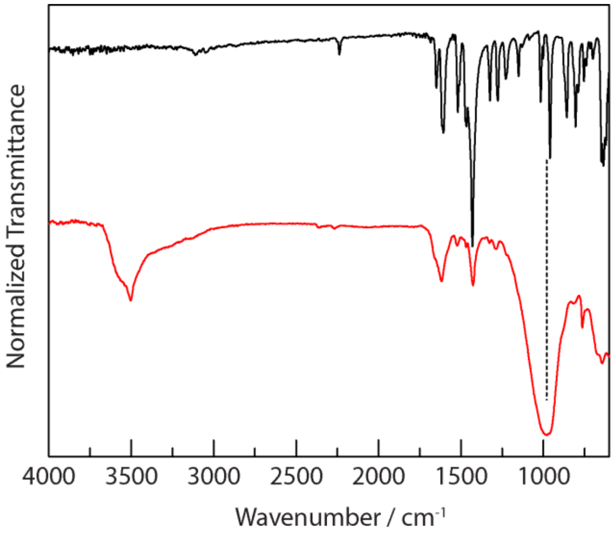

Figure S5. IR spectra of Ru$_2$(4-CN-hp)$_4$Cl (**1e**, —) and Ru$_2$(4-CN-hp)$_4$BF$_4$ (**2e**, —). The characteristic B–F stretching frequency of tetrafluoroborate anion (broad ~1020 cm^{-1}) is observed after treatment of **1e** with AgBF$_4$.

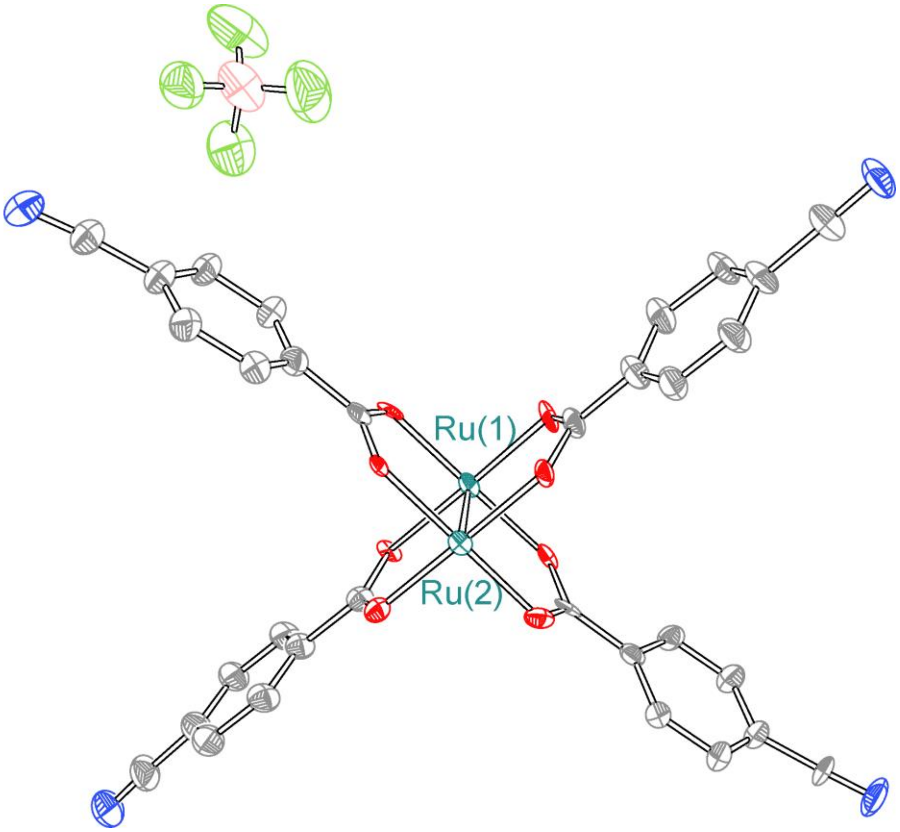

Figure S6. Thermal ellipsoid plot of $Ru_2(4\text{-}CN\text{-}OBz)_4BF_4$ (**2a**) drawn at the 50% probability level. H-atoms and solvent molecules are removed for clarity.

Table S1. Crystal data and structure refinement for $Ru_2(4\text{-CN-OBz})_4BF_4$ (**2a**, CCDC 2011433).

Crystal data	
Chemical formula	$C_{32}H_{20}N_4O_{10}Ru_2 \cdot BF_4 \cdot 4(C_3H_6O)$
Fw (g/mol)	1141.78
Temperature (K)	110(2)
Crystal system, space group	Monoclinic, $P2_1/n$
a, b, c (Å)	17.05(1), 16.73(1), 19.52(1)
α, β, γ (°)	90, 92.238(8), 90
V (Å^3)	5563(6)
Z	4
Radiation type	Mo Kα radiation, λ = 0.71073 Å
μ (mm^{-1})	0.62
Crystal size (mm)	0.01 × 0.01 × 0.01
Data collection	
Diffractometer	Bruker APEX-II CCD
Absorption correction	Multi-scan, *SADABS*
No. of measured, independent and observed [I>2σ (I)] reflections	23018, 3847, 1992
R_{int}	0.184
$\sin(\theta/\lambda)_{max}$ (Å^{-1})	0.436
Refinement	
$R[F^2 > 2\sigma(F^2)]$, $wR(F^2)$, S	0.069, 0.252, 0.99
No. of reflections	3847
No. of parameters	633
No. of restraints	887
H-atom treatment	H-atom parameters constrained
r_{max}, r_{min} (e Å^{-3})	1.19, –0.81

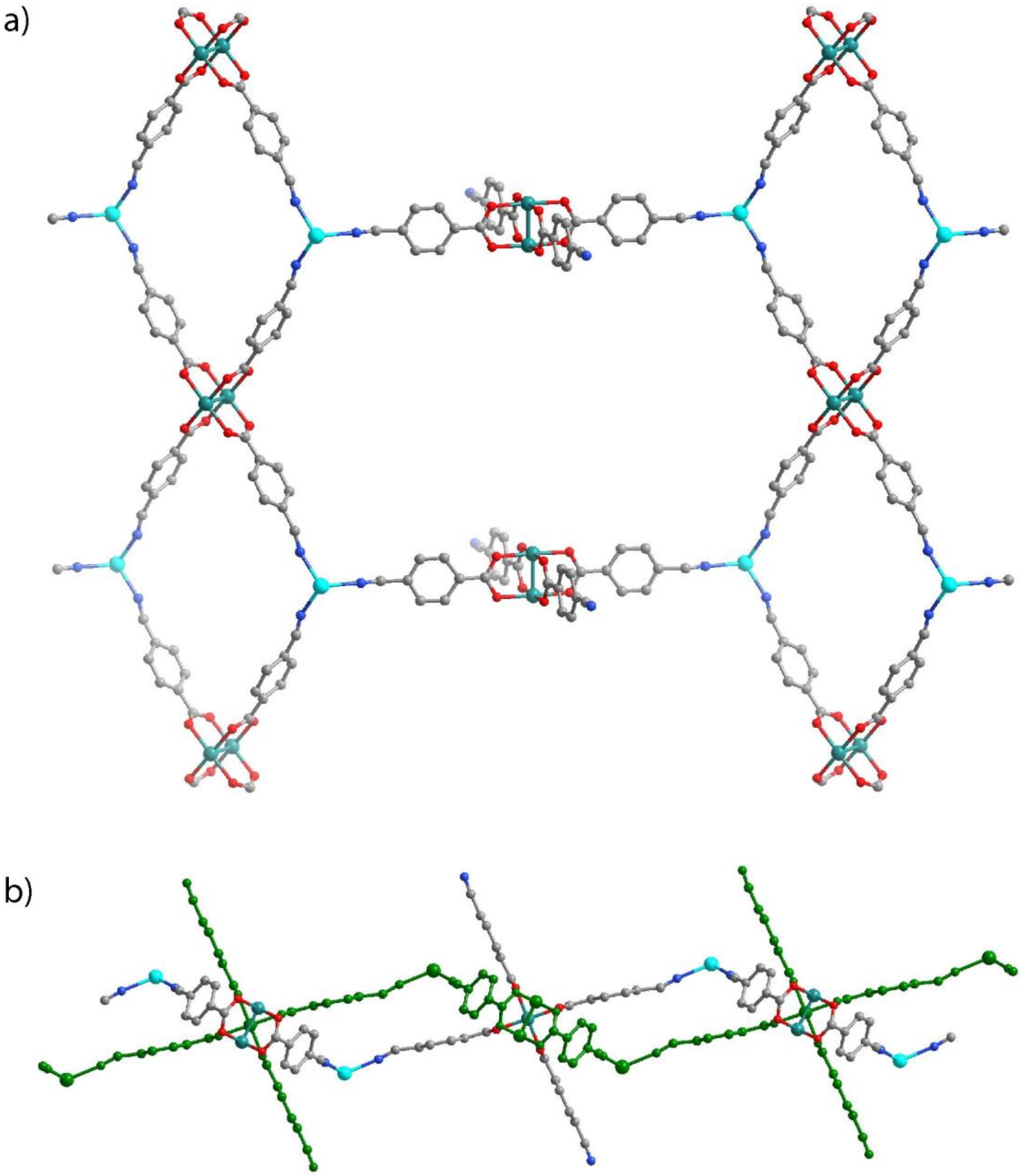

Figure S7. a) The two-dimensional (2-D) structure of [Ag(**2a**)OTf]. The 2-D layer without interpenetration is presented here. b) The 2-fold interpenetrated coordination polymer is viewed from *b* axis. The non-coordinated nitrile groups are visible in this direction.

Table S2. Crystal data and structure refinement for [Ag(**2a**)OTf] (CCDC 2011431).

Crystal data	
Chemical formula	0.5($C_{64}H_{32}Ag_2N_8O_{20}Ru_4$)
Fw (g/mol)	926.50
Temperature (K)	110(2)
Crystal system, space group	Monoclinic, *P*2/*m*
a, *b*, *c* (Å)	12.455(5), 19.023(8), 16.766(7)
α, β, γ (°)	90, 97.049(5), 90
V ($Å^3$)	3942(3)
Z	2
Radiation type	Mo Kα radiation, λ = 0.71073 Å
μ (mm^{-1})	0.65
Crystal size (mm)	0.01 × 0.01 × 0.01
Data collection	
Diffractometer	Bruker APEX-II CCD
Absorption correction	Multi-scan, *SADABS*
No. of measured, independent and observed [I>2σ (I)] reflections	13095, 3645, 2049
R_{int}	0.056
$\sin(\theta/\lambda)_{\max}$ ($Å^{-1}$)	0.476
Refinement	
$R[F^2 > 2\sigma(F^2)]$, $wR(F^2)$, S	0.141, 0.487, 1.79
No. of reflections	3645
No. of parameters	230
No. of restraints	373
H-atom treatment	H-atom parameters constrained
$r_{\max}$, $r_{\min}$ (e $Å^{-3}$)	3.45, −1.51

Table S3. Crystal data and structure refinement for [Ag_2(**2b**)$(OTf)_2$] (CCDC 2011428).

Crystal data	
Chemical formula	$C_{19}H_{14}AgN_2O_5Ru$
Fw (g/mol)	559.26
Temperature (K)	110(2)
Crystal system, space group	Triclinic, $P\bar{1}$
a, b, c (Å)	9.906(9), 10.76(1), 13.97(1)
α, β, γ (°)	88.37(1), 80.63(1), 86.79(1)
V ($Å^3$)	1466(2)
Z	2
Radiation type	Mo Kα radiation, λ = 0.71073 Å
μ (mm^{-1})	1.20
Crystal size (mm)	0.02 × 0.02 × 0.01
Data collection	
Diffractometer	Bruker APEX-II CCD
Absorption correction	Multi-scan, *SADABS*
No. of measured, independent and observed [$I>2\sigma(I)$] reflections	9157, 3528, 1994
R_{int}	0.108
$\sin(\theta/\lambda)_{max}$ ($Å^{-1}$)	0.524
Refinement	
$R[F^2 > 2\sigma(F^2)]$, $wR(F^2)$, S	0.069, 0.227, 1.08
No. of reflections	3528
No. of parameters	232
No. of restraints	84
H-atom treatment	H-atom parameters constrained
r_{max}, r_{min} (e $Å^{-3}$)	0.76, −0.92

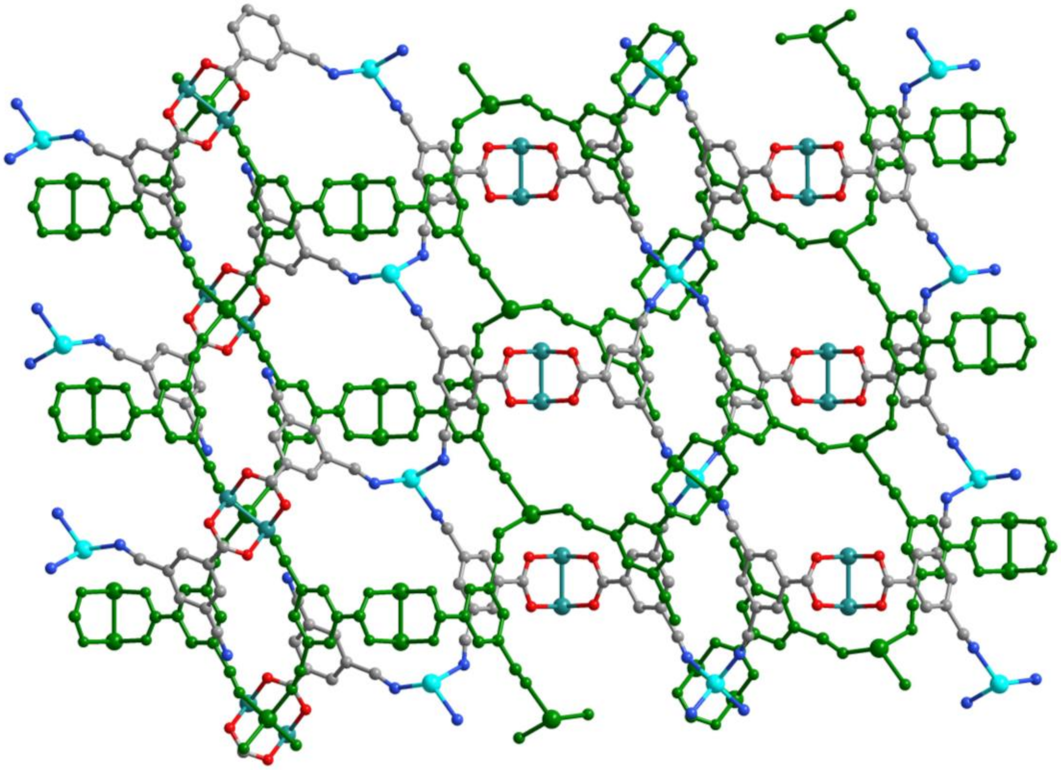

Figure S8a. An extended network structure of [Ag_2(**2c**)(OTf)$_2$] viewed from *b* axis with the interpenetration, which is marked green.

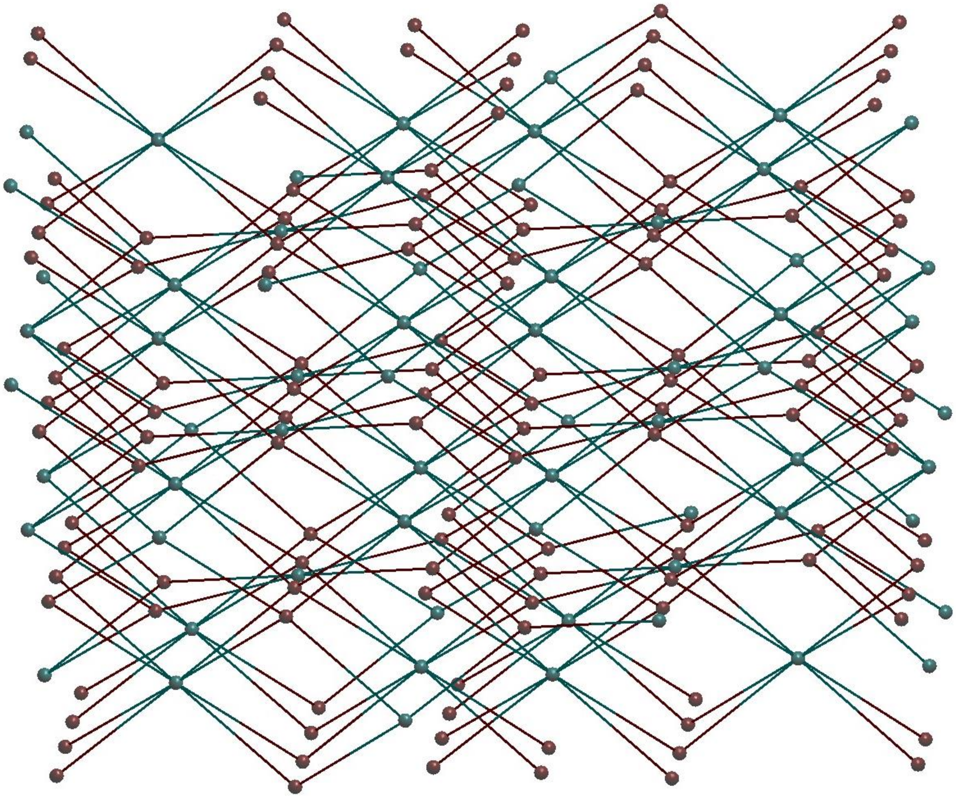

Figure S8b. [Ag_2(**2c**)$(OTf)_2$] is described as a new 3,4,4,8-connected (4 nodal) net topology with point symbol as $(4^2.6)_4(4^2.8^4)(4^6)(4^9.6^{10}.8^9)_2$, if the two types of metallomonomers are simplified as 8-connected and 4-connected nodes and the two kinds of Ag(I) ions serve as 3-connected and 4-connected nodes.

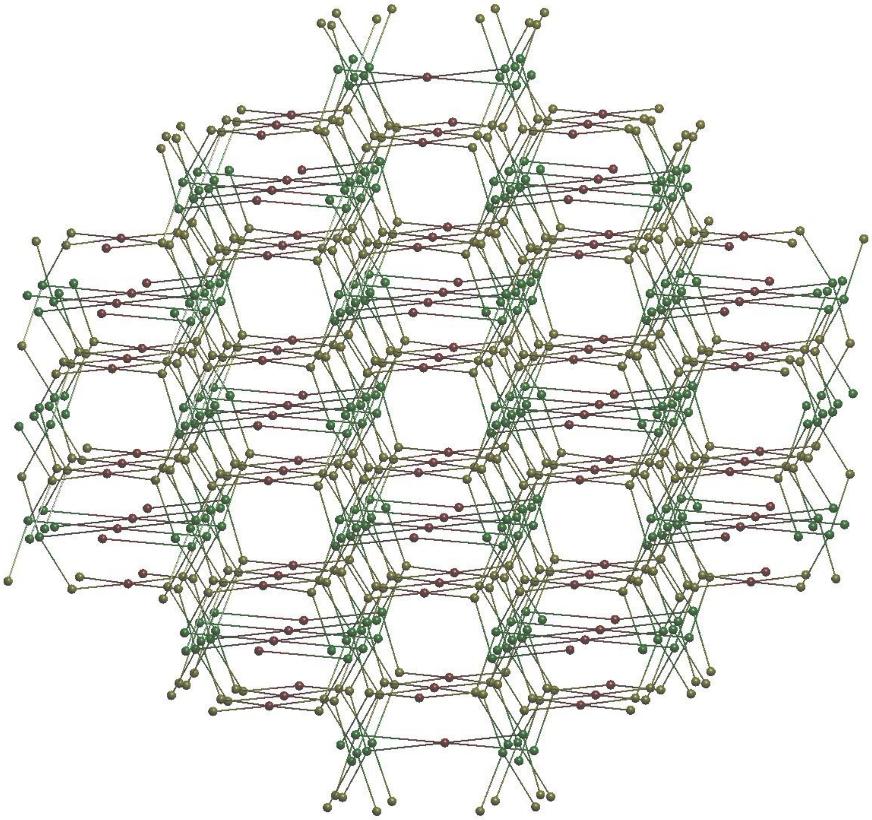

Figure S8c. [Ag_2(**2c**)(OTf)$_2$] can also be described as a new 3,3,3,4,4,4-connected (6-nodal) net topology with point symbol as $(4.8^2)_4(4^2.8^4)_2(6.8^2)_8(6.8^3.10^2)_2(6^2.8^2.10^2)$, if Ru_2 cores are simplified as 4-connected nodes, 3,5-dicyanobenzoate ligands as 3-connected nodes, and the two kinds of Ag(I) ions as 3-connected and 4-connected nodes.

Table S4. Crystal data and structure refinement for [Ag_2(**2c**)$(OTf)_2$] (CCDC 2011430).

Crystal data	
Chemical formula	$0.17(C_{216}H_{72}Ag_{12}N_{48}O_{60}Ru_{12})\cdot 2(C_{0.33}FOS_{0.33})$
Fw (g/mol)	1233.80
Temperature (K)	110(2)
Crystal system, space group	Monoclinic, *C*2/*m*
a, *b*, *c* (Å)	18.862(2), 26.135(3), 20.514(2)
α, β, γ (°)	90, 91.362(2), 90
V ($Å^3$)	10110(2)
Z	6
Radiation type	Synchrotron radiation, $\lambda = 0.41328$ Å
μ (mm^{-1})	1.42
Crystal size (mm)	0.02 × 0.02 × 0.01
Data collection	
Diffractometer	Pilatus3 X CdTe 1M
Absorption correction	Multi-scan, *SADABS*
No. of measured, independent and observed [$I>2\sigma(I)$] reflections	73623, 6171, 4119
R_{int}	0.094
$\sin(\theta/\lambda)_{\text{max}}$ ($Å^{-1}$)	0.522
Refinement	
$R[F^2 > 2\sigma(F^2)]$, $wR(F^2)$, S	0.121, 0.383, 1.51
No. of reflections	6171
No. of parameters	454
No. of restraints	8
H-atom treatment	H-atom parameters constrained
r_{max}, r_{min} (e $Å^{-3}$)	2.80, −0.97

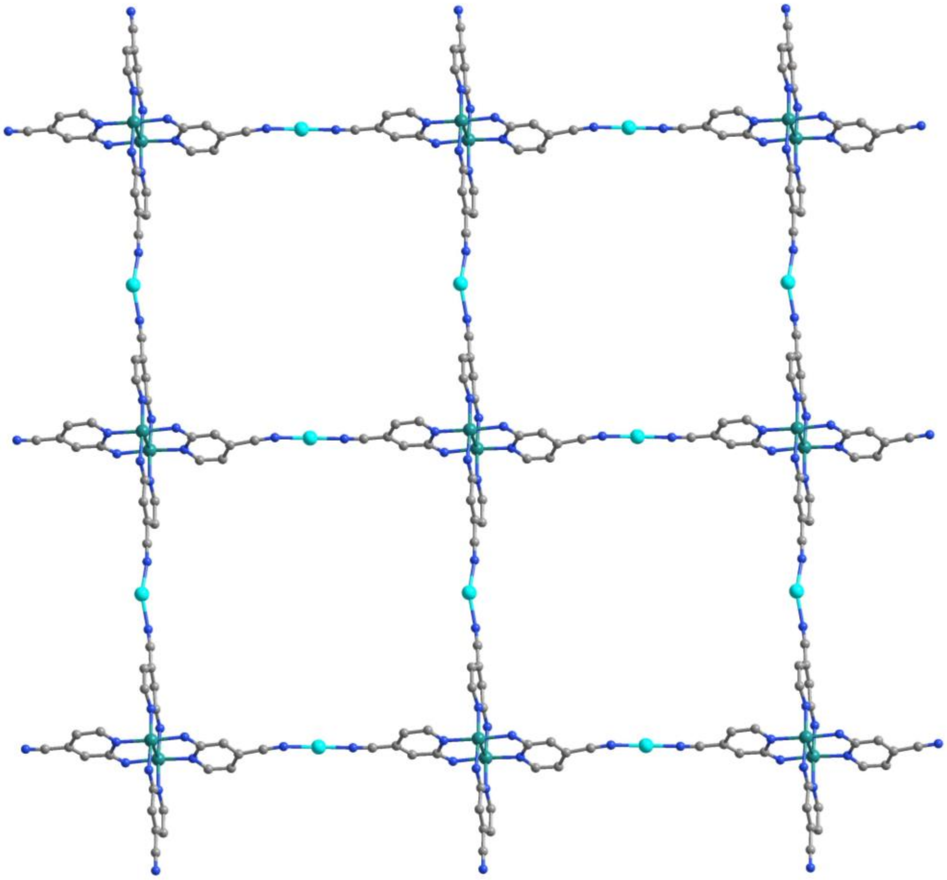

Figure S9. The extended 2-dimensional network of [Ag_2(**2d**)($OTf)_2$]. The triflate anions and H-atoms are omitted in the above figure for clarity. Topologically, [Ag_2(**2d**)($OTf)_2$] is described as a **sql** net, in which each metallomonomer serves as a 4-connected node.

Table S5. Crystal data and structure refinement for [Ag_2(**2d**)$(OTf)_2$] (CCDC 2011429).

Crystal data	
Chemical formula	$C_{25.58}H_{16}Ag_2F_{4.75}N_{12}O_{6.75}Ru_2S_{1.58}\cdot0.5(CF_3O_3S)$
Fw (g/mol)	1232.95
Temperature (K)	110(2)
Crystal system, space group	Monoclinic, *C*2/*c*
a, *b*, *c* (Å)	27.33(1), 26.528(9), 19.548(7)
α, β, γ (°)	90, 119.316(5), 90
V (Å^3)	12356(8)
Z	8
Radiation type	Mo Kα radiation, λ = 0.71073 Å
μ (mm^{-1})	1.23
Crystal size (mm)	0.01 × 0.01 × 0.01
Data collection	
Diffractometer	Bruker APEX-II CCD
Absorption correction	Multi-scan, *SADABS*
No. of measured, independent and observed [I>2σ (I)] reflections	29535, 3370, 1952
R_{int}	0.135
$\sin(\theta/\lambda)_{\text{max}}$ (Å^{-1})	0.404
Refinement	
$R[F^2 > 2\sigma(F^2)]$, $wR(F^2)$, S	0.120, 0.383, 1.43
No. of reflections	3370
No. of parameters	587
No. of restraints	849
H-atom treatment	H-atom parameters constrained
r_{max}, r_{min} (e Å^{-3})	2.04, –1.48

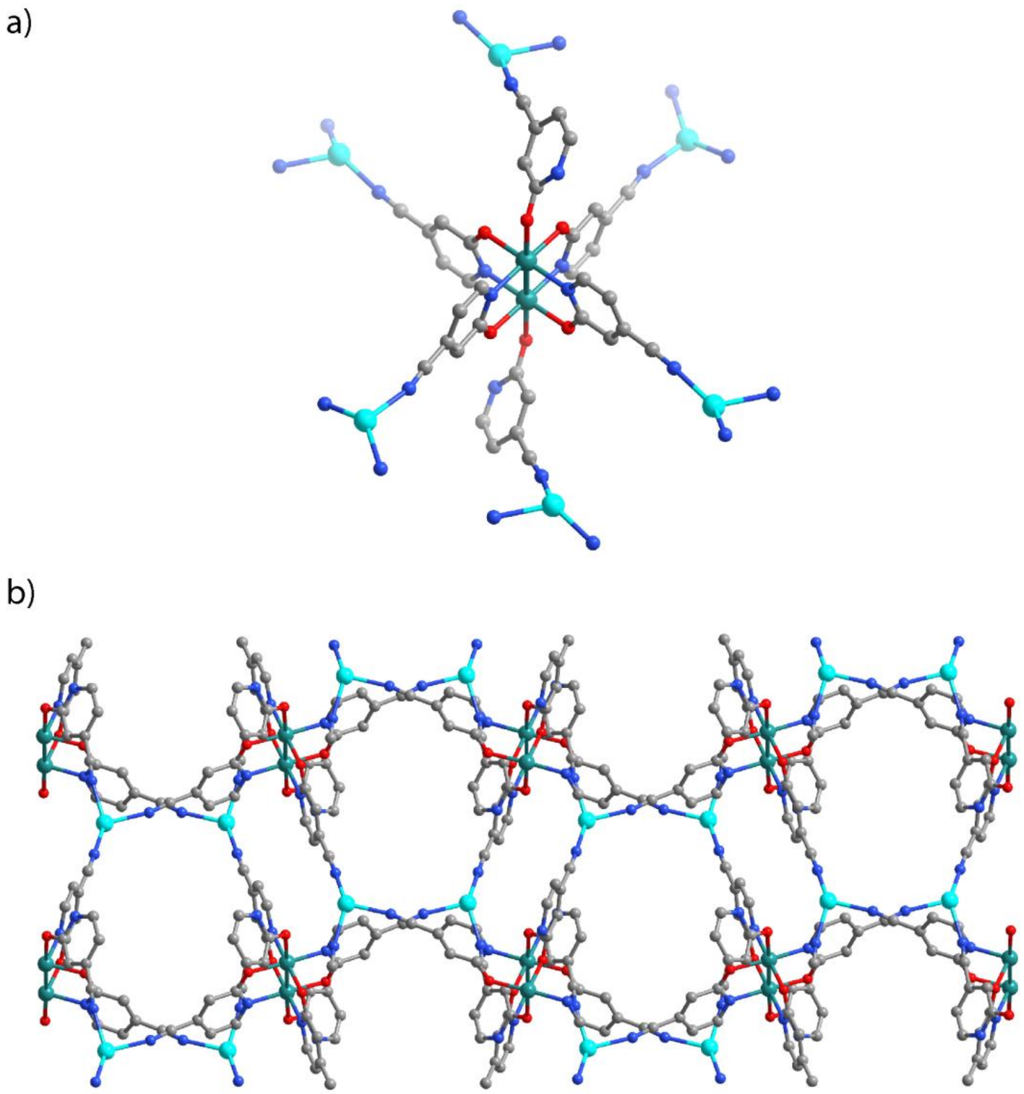

Figure S10. a) The metalloligand **2e** coordinates to six Ag(I) nodes. b) The extended 3-dimensional network of [Ag_2(**2e**)$(OTf)_2$]. The triflate anions and H-atoms are omitted in the above figure for clarity. Topologically, [Ag_2(**2e**)$(OTf)_2$] is described as a 3,6-connected **rtl** net, in which each Ag(I) ion serves as a 3-connected node and each metallomonomer serves as a 6-connected node.

Table S6. Crystal data and structure refinement for [Ag_2(**2e**)$(OTf)_2$] (CCDC 2011432).

Crystal data	
Chemical formula	$0.5(C_{76}H_{36}Ag_4F_{12}N_{24}O_{24}Ru_4S_4)$
Fw (g/mol)	1430.64
Temperature (K)	110(2)
Crystal system, space group	Monoclinic, $P2_1/c$
a, b, c (Å)	11.146(2), 23.537(4), 11.624(2)
α, β, γ (°)	90, 94.558(4), 90
V (Å^3)	3040.0(8)
Z	2
Radiation type	Mo Kα radiation, λ = 0.71073 Å
μ (mm^{-1})	1.27
Crystal size (mm)	0.01 × 0.01 × 0.01
Data collection	
Diffractometer	Bruker Quest CPAD detector
Absorption correction	Multi-scan, *SADABS*
No. of measured, independent and observed [I>2σ (I)] reflections	31870, 3190, 2299
R_{int}	0.175
$\sin(\theta/\lambda)_{\text{max}}$ (Å^{-1})	0.501
Refinement	
$R[F^2 > 2\sigma(F^2)]$, $wR(F^2)$, S	0.072, 0.176, 1.05
No. of reflections	3190
No. of parameters	334
No. of restraints	469
H-atom treatment	H-atom parameters constrained $w = 1/[\sigma^2(F_o^2) + (0.0685P)^2 + 31.7713P]$ where $P = (F_o^2 + 2F_c^2)/3$
r_{max}, r_{min} (e Å^{-3})	1.73, –1.38

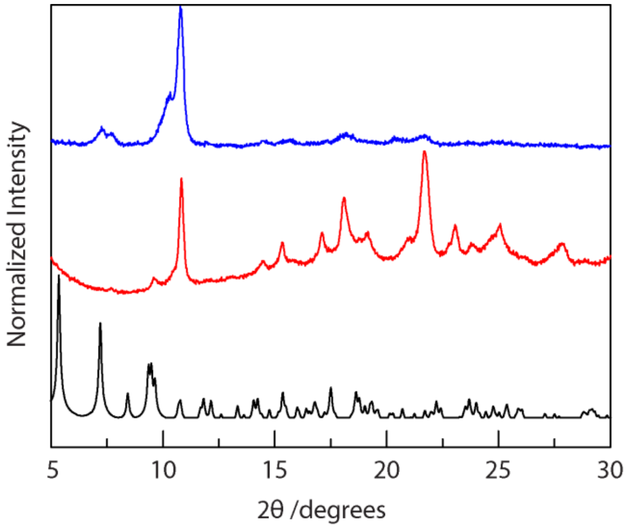

Figure S11. PXRD patterns of the heterobimetallic coordination polymer [Ag(**2a**)OTf] (—, calculated), a sample collected using gas-tight PXRD holder (—), and the sample upon losing the mother liquid (—). These data indicate that heterobimetallic MOF [Ag(**2a**)OTf] collapses upon desolvation.

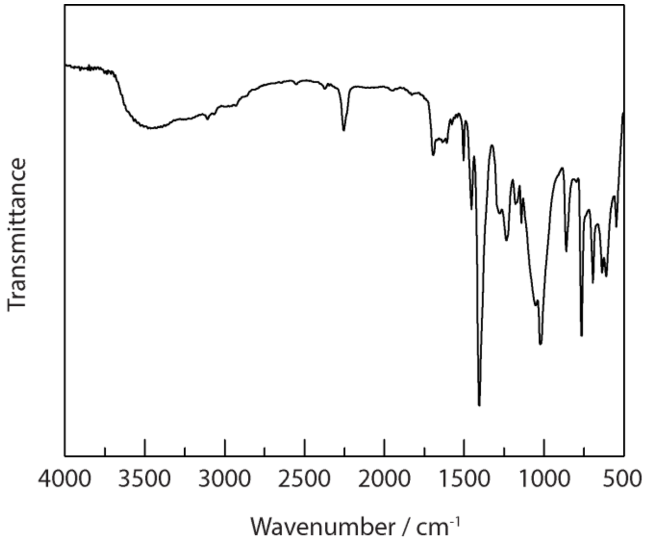

Figure S12a. IR spectrum of [Ag(**2a**)OTf] (**—**). The characteristic peaks of tetrafluoroborate anion (B–F asymmetric stretching at ~1020 cm^{-1}) and triflate anion (CF_3 symmetric stretching at ~1225 cm^{-1}; SO_3 asymmetric stretching at ~1275 cm^{-1}) are observed.

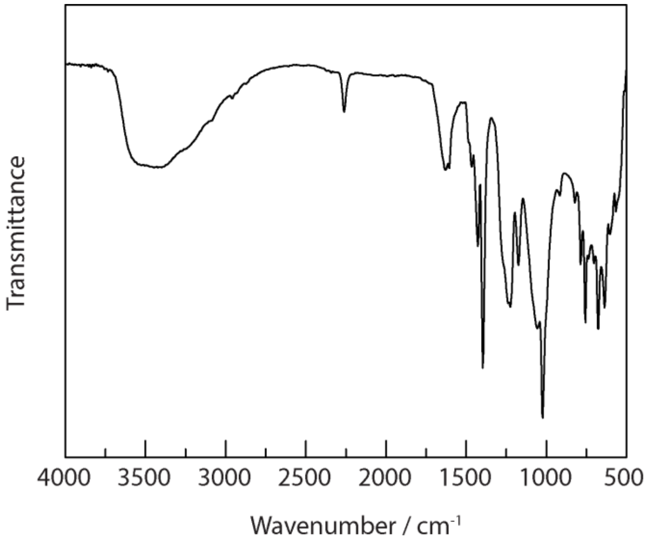

Figure S12b. IR spectrum of [Ag_2(**2b**)$(OTf)_2$] (**—**). The characteristic peaks of tetrafluoroborate anion (B–F asymmetric stretching at ~1020 cm^{-1}) and triflate anion (CF_3 symmetric stretching at ~1225 cm^{-1}; SO_3 asymmetric stretching at ~1275 cm^{-1}) are observed.

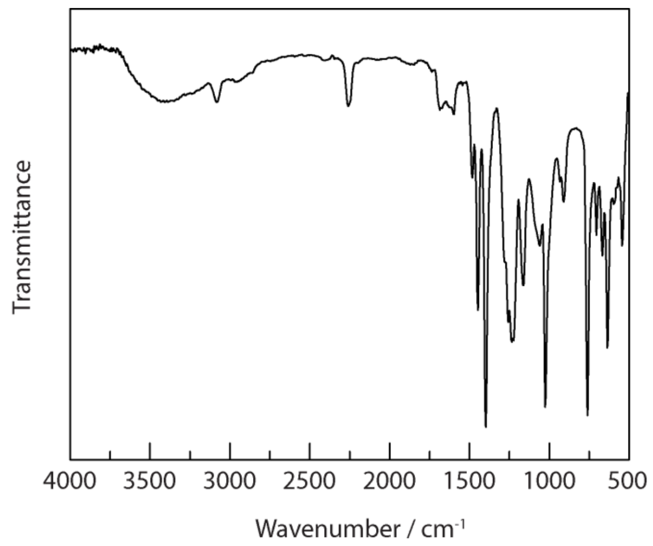

Figure S12c. IR spectrum of [Ag_2(**2c**)$(OTf)_2$] (**—**). The characteristic peaks of tetrafluoroborate anion (B–F asymmetric stretching at ~1020 cm^{-1}) and triflate anion (CF_3 symmetric stretching at ~1225 cm^{-1}; SO_3 asymmetric stretching at ~1275 cm^{-1}) are observed.

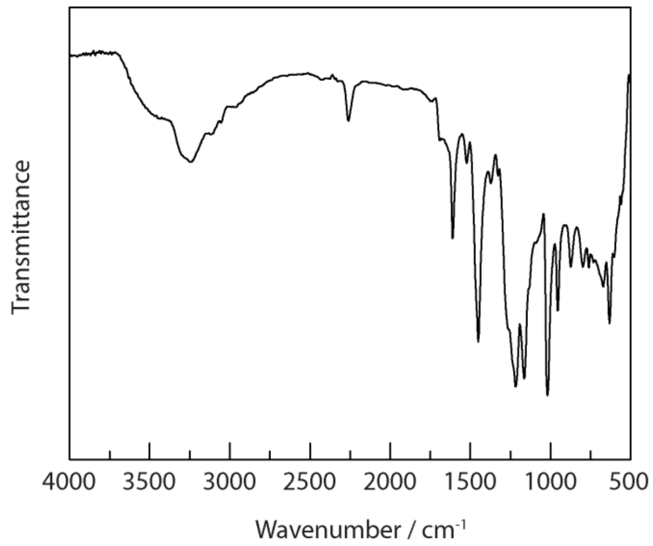

Figure S12d. IR spectrum of [Ag_2(**2d**)$(OTf)_2$] (—). The characteristic peaks of tetrafluoroborate anion (B–F asymmetric stretching at ~1020 cm^{-1}) and triflate anion (CF_3 symmetric stretching at ~1225 cm^{-1}; SO_3 asymmetric stretching at ~1275 cm^{-1}) are observed.

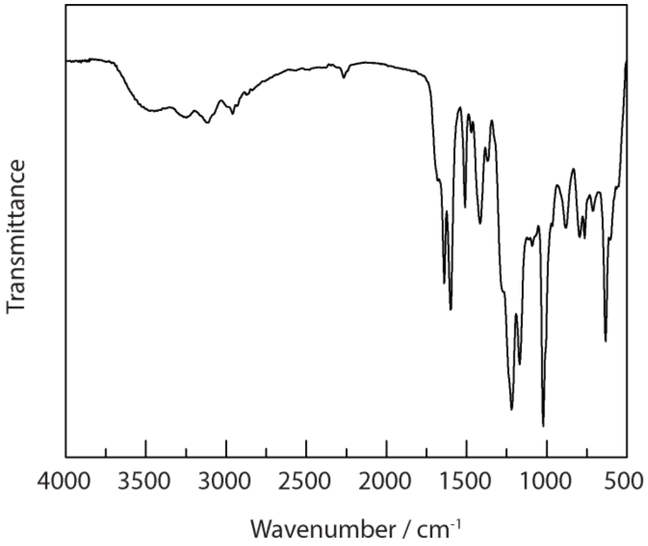

Figure S12e. IR spectrum of [Ag_2(**2e**)$(OTf)_2$] (—). The characteristic peaks of tetrafluoroborate anion (B–F asymmetric stretching at ~1020 cm^{-1}) and triflate anion (CF_3 symmetric stretching at ~1225 cm^{-1}; SO_3 asymmetric stretching at ~1275 cm^{-1}) are observed.

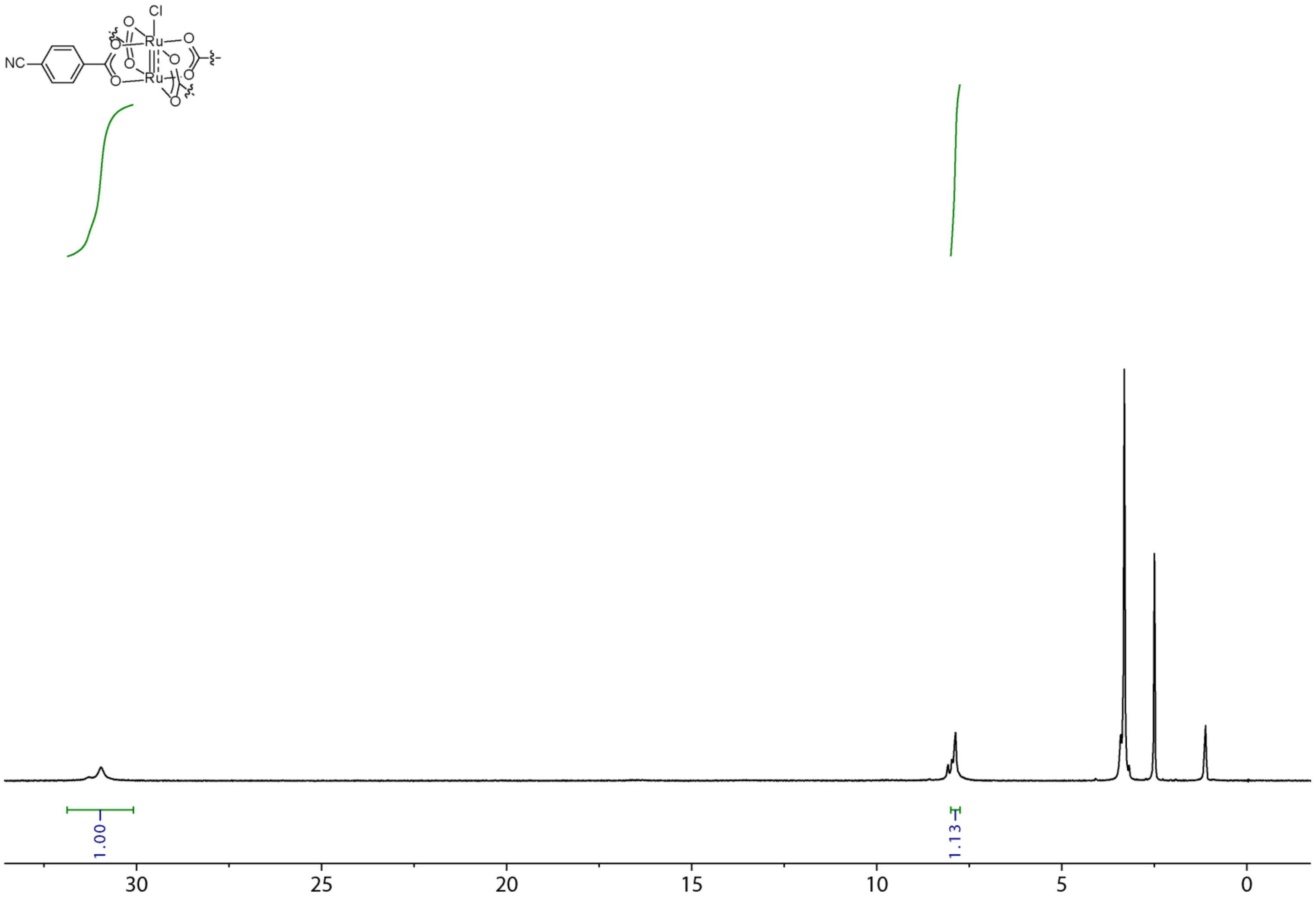

Figure S13. ^{1}H NMR spectrum of **1a** acquired at 23 °C in d_6-DMSO.

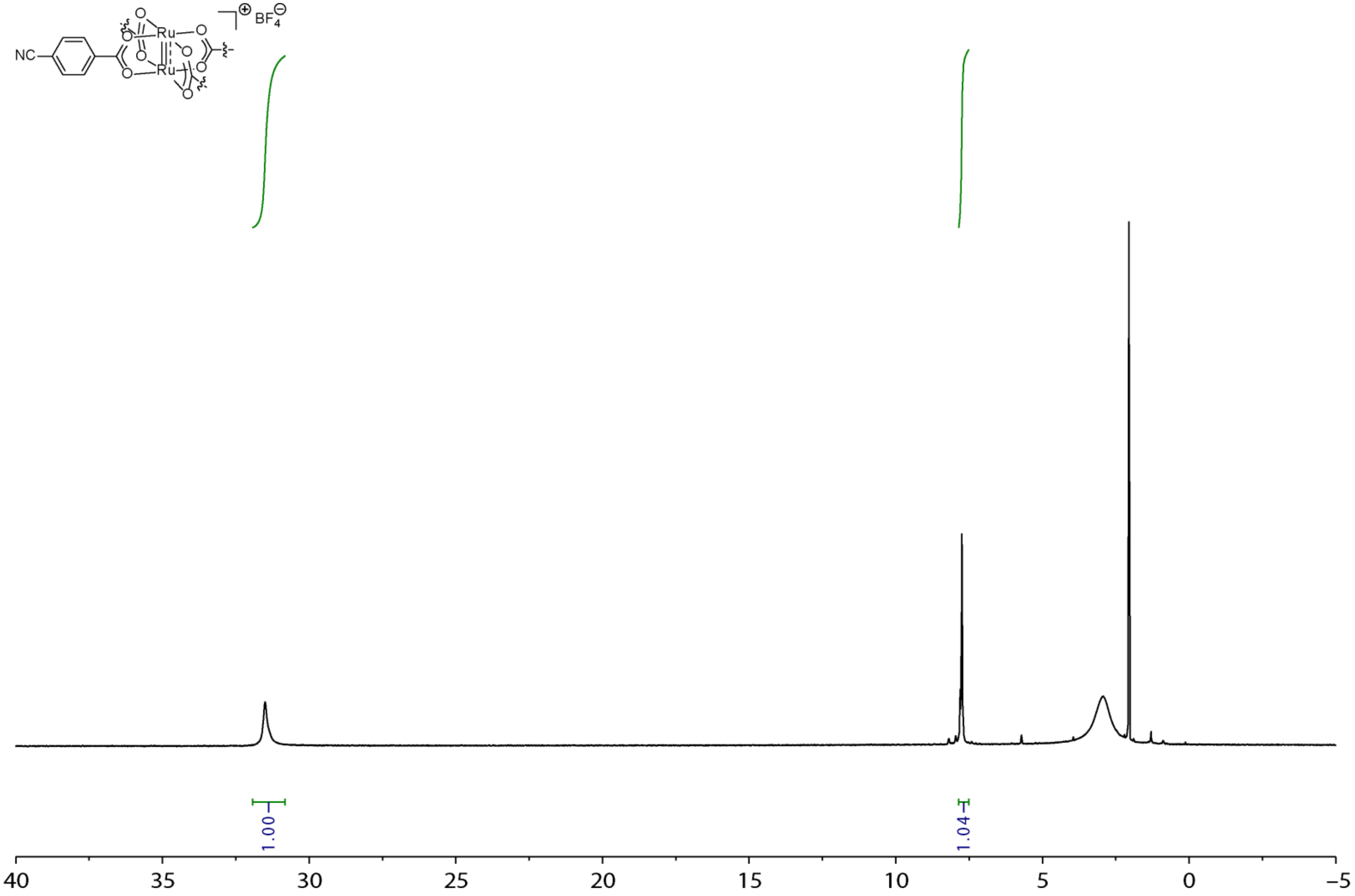

Figure S14. ^{1}H NMR spectrum of **2a** acquired at 23 °C in *d*$_6$-acetone.

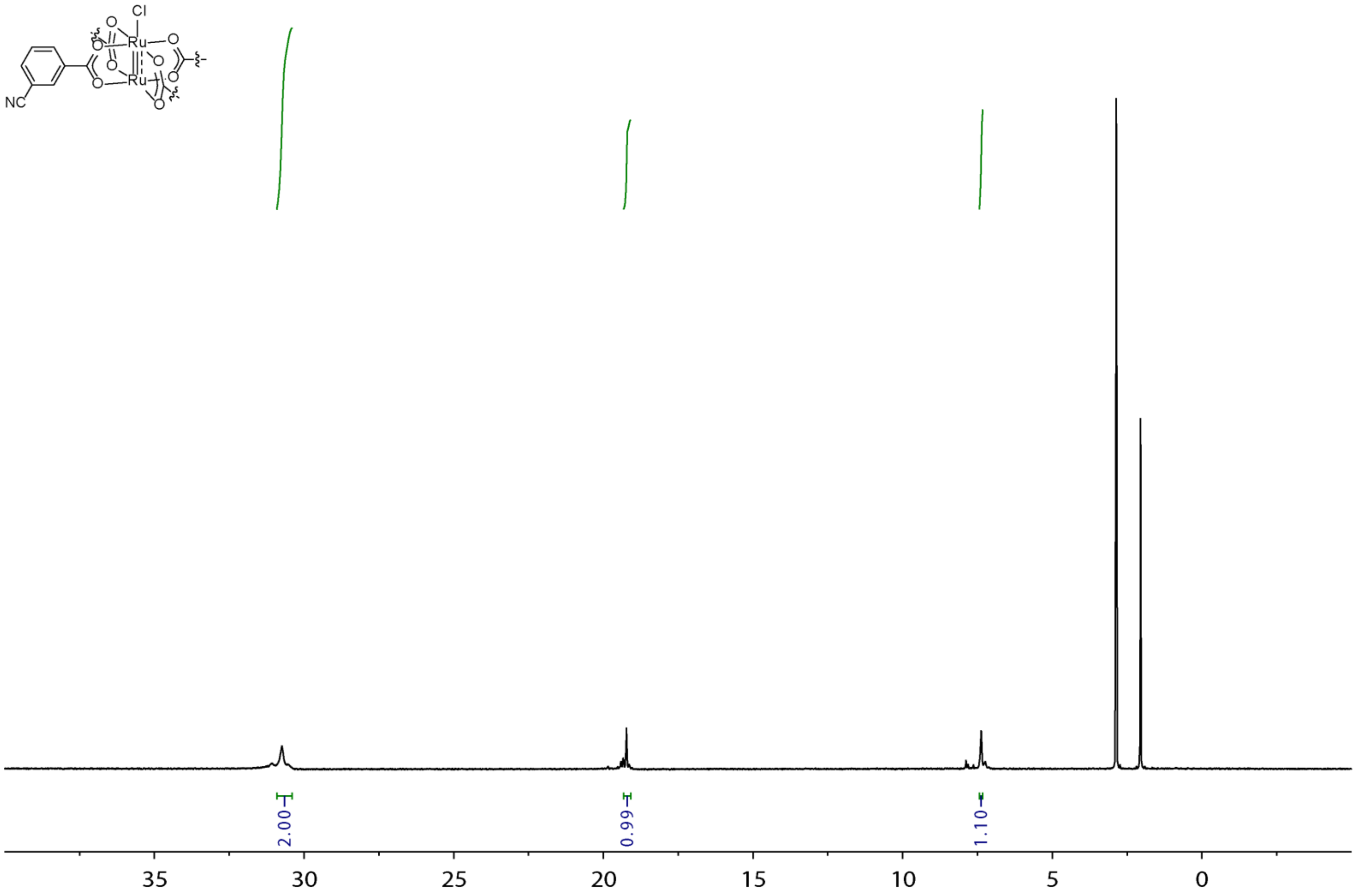

Figure S15. ^{1}H NMR spectrum of **1b** acquired at 23 °C in d_6-DMSO.

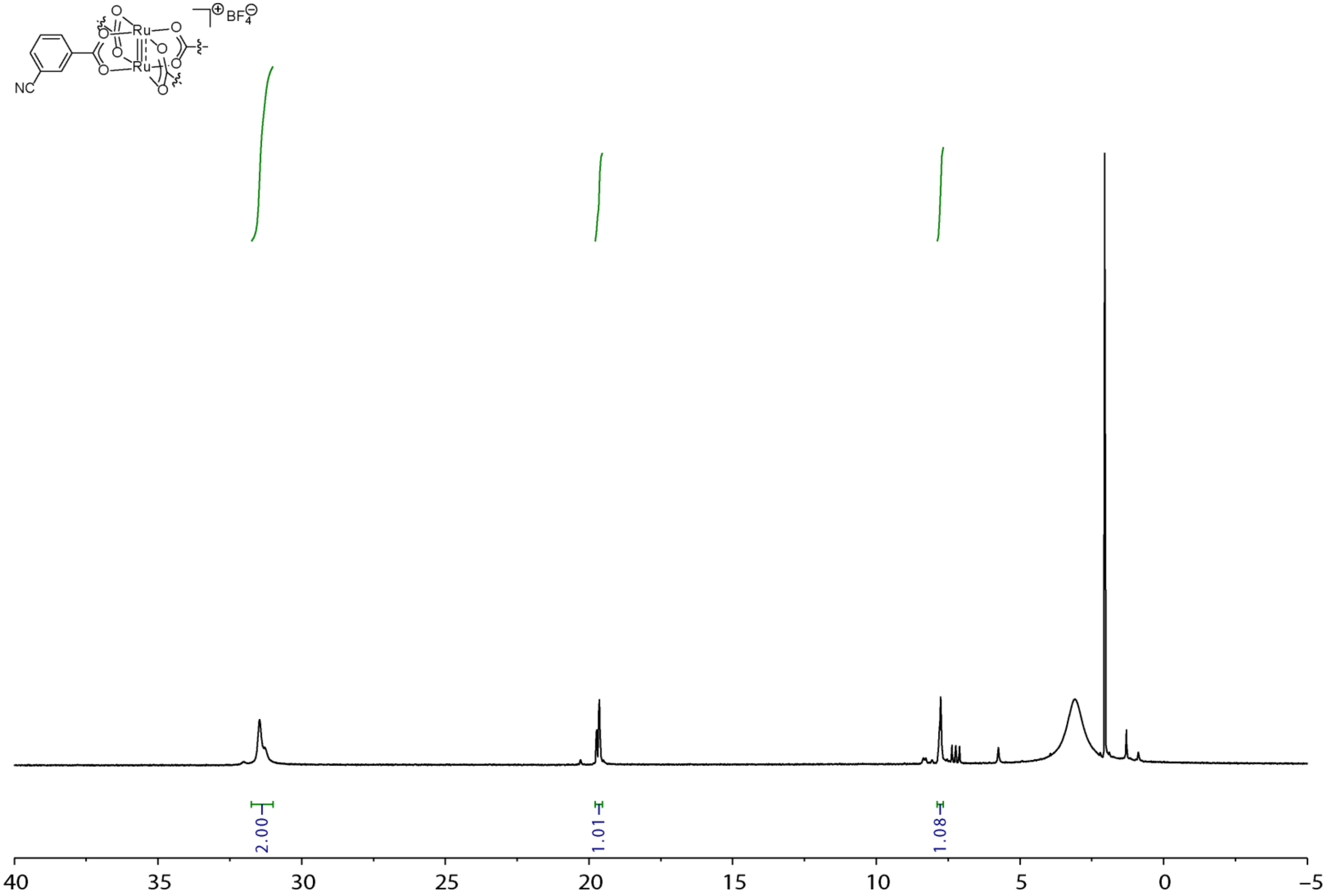

Figure S16. ^{1}H NMR spectrum of **2b** acquired at 23 °C in *d*$_6$-acetone.

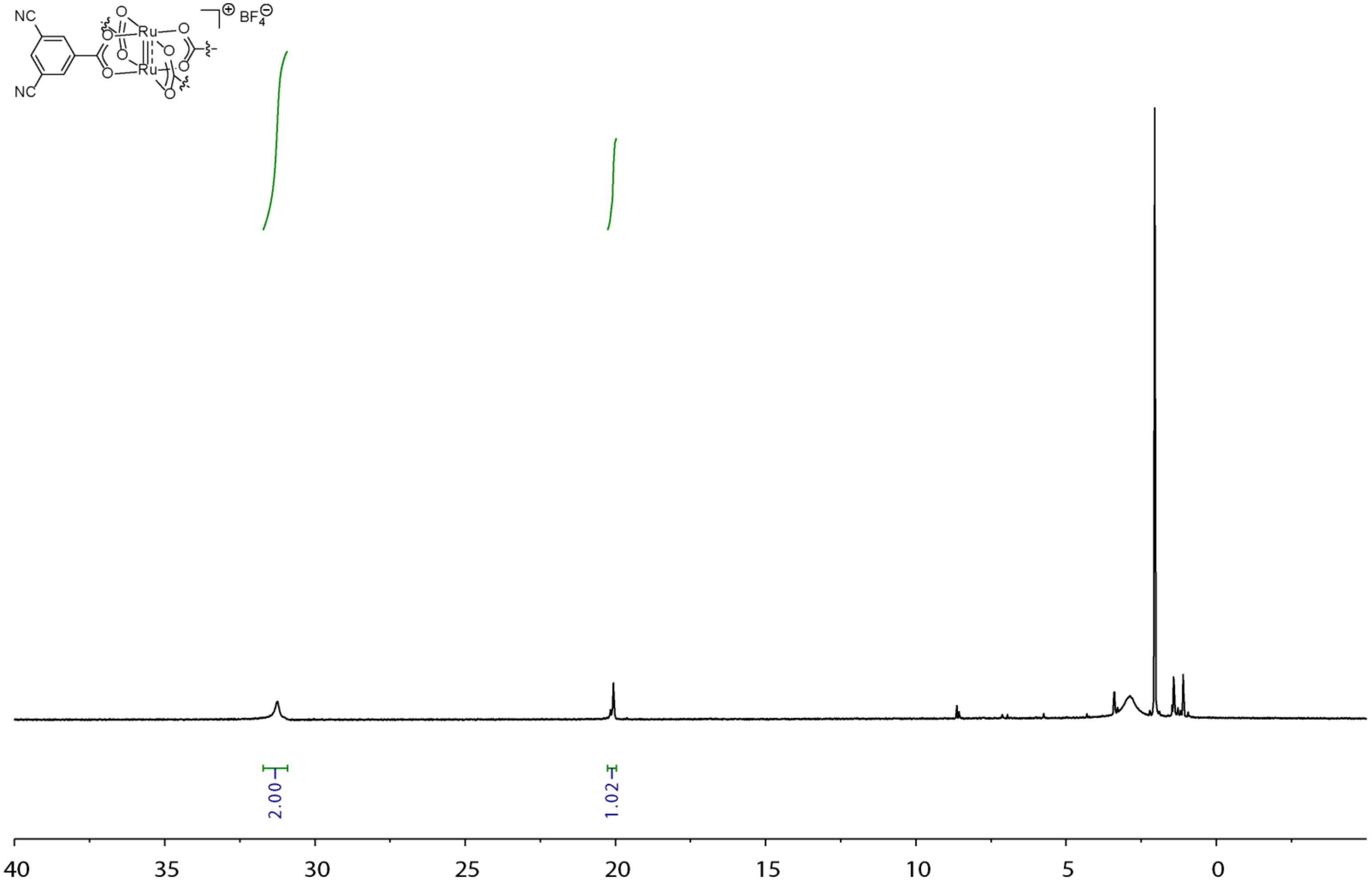

Figure S17. ^{1}H NMR spectrum of **2c** acquired at 23 °C in *d*$_6$-acetone.

D. References

1. Wang, C.-H.; Das, A.; Gao, W.-Y.; Powers, D. C. *Angew. Chem. Int. Ed.* **2018**, *57*, 3676–3681.
2. Baloglu, E.; Ghosh, S.; Lobera, M.; Schmidt, D. International Bureau WO 2011/088181 A1, 21 July 2011.
3. Fulmer, G. R.; Miller, A. J. M.; Sherden, N. H.; Gottlieb, H. E.; Nudelman, A.; Stoltz, B. M.; Bercaw, J. E.; Goldberg, K. I. *Organometallics* **2010**, *29*, 2176–2179.
4 Sheldrick, G. M. SADABS Program for Absorption Correction for Data of Area Detector Frame. BRUKER AXS Inc., 5465 East Cheryl Parkway, Madison, WI 53711–5373, USA, 2000.
5. Sheldrick, G. M. *Acta Crystallogr., Sect. A* **2008,** *64*, 112–122.
6. Sheldrick, G. M. *Acta Crystallogr., Sect. C* **2015,** *71*, 3–8.
7. Dolomanov, O. V.; Bourhis, L. J.; Gildea, R. J.; Howard, J. A. K.; Puschmann, H. *J. Appl. Crystallogr.* **2009,** *42*, 339–341.
8. Macrae, C. F.; Edgington, P. R.; McCabe, P.; Pidcock, E.; Shields, G. P.; Taylor, R.; Towler, M.; van de Streek, J. *J. Appl. Crystallogr.* **2006,** *39*, 453–457.